

# Rate Adaptive Coded Digital Phase Modulation

Yang Liu, Zihuai Lin

School of Electrical and Information Engineering, University of Sydney, NSW 2006,  
Australia

E-mail: zihuai.lin@sydney.edu.au

## Abstract

In this paper, rate adaptive coded Digital Phase Modulation (DPM) schemes based on punctured ring convolutional codes are presented. We first present an upper bound on symbol error probability for punctured convolutional coded Continuous Phase Modulation (CPM) over rings with Maximum Likelihood Sequence Detection (MLSD). The bound is based on the transfer function technique, which is modified and generalized to punctured convolutional codes over rings. The novelty of this paper is the development of the analytical upper bound on the symbol error probability for the investigated system. This work provides a systematic way to analyze and design the rate adaptive ring convolutional coded CPM systems. The analysis method is very general. It may be applied to any trellis based coding schemes.

## I. INTRODUCTION

Trellis coded Continuous Phase Modulation (CPM) is a bandwidth and power efficient coded modulation scheme [1]. It has been studied in the past decades [1–3]. One of the advantages of trellis coded CPM is its constant envelope property, which makes it a very suitable choice for data transmissions over nonlinear and/or fading channels, *e.g.*, satellite and radio communication channels. This is because it can minimize the distortion due to non-linear amplification in the high power amplifiers. power amplifiers can be used, which can save 3 – 10 dB losses of non-linear distortion [1]. higher power efficiency. Because of the constant envelope property, these schemes are mostly suitable for fading channels, such as satellite and mobile radio channels. We investigate a coded modulation scheme based on non-binary trellis encoders, particularly, on ring convolutional encoders [4, 5]. The concept of convolutional codes over rings is first introduced by Massey and Mittelholzer *et al* in [4, 5]. They show that when combined with  $M$ -ary phase modulation, with the same number of states, convolutional codes over the ring of integers modulo- $M$  have at least as large a free Euclidean distance [6] as the best binary convolutional codes on the Galois field  $GF(2)$ .

The applications of such schemes are for data transmissions over nonlinear and/or fading channels, *e.g.*, satellite and radio communication channels. schemes are usually considered as the most suitable choice. Phase Shift Keying (PSK), which has been widely used *e.g.*, [7], also has constant envelope. But the discontinuous phase change between adjacent channel symbols results in energy inefficiency. CPM has not only constant envelope but also continues phase changes. Compared with PSK, CPM has less energy in its side lobe in their spectra, thus is more spectra efficient.

Due to the excellent bandwidth efficiency, some non-constant envelope schemes, *e.g.*,  $Q^2$ PSK, SQAM [8], can also be applicable to satellite communications. In this case, however, the Traveling Wave Tube (TWT) type amplifier, which is currently used in communication satellite transponders and exhibit non-linear characteristics in both amplitude and phase of the signal, must operate in the linear region [8]. This will increase the system complexity and a significant loss of transmitter power.

The concept of convolutional codes over rings is firstly introduced by Massey and Mittelholzer *et al* in [4]. They show that when combined with  $M$ -ary phase modulation, with the same number of states, convolutional codes over the ring of integers modulo- $M$  have at least as large a free Euclidean distance [1] as the best binary convolutional codes on the Galois field  $GF(2)$ . It is shown [2, 3] that compared to trellis coded CPM systems using binary codes of the same complexity, ring convolutional coded CPM yield larger minimum normalized squared Euclidean distance [1].

Most of the previous works in the area of ring convolutional coded CPM, *e.g.*, [2, 3, 9], focus on searching

convolutional coded CPFSK [1]<sup>1</sup> schemes are used for MPEG-4 image transmission. There, Maximum *a posteriori* (MAP) sequence detection (based on the Viterbi algorithm [11]), is used for the recovery of the binary bit streams from the MPEG-4 encoder. Serially concatenated CPM with a ring convolutional encoder as the outer encoder is investigated in [12]. In this paper, we investigate rate flexible coded CPM over rings using Punctured Ring Convolutional Codes (PRCC). With adaptive coded CPM, the channel coding rate can be adapted to the channel condition, therefore, the proposed scheme is more robust compared with fixed rate coded CPM schemes.

For the un-interleaved PRCC/CPM scheme, an analytical upper bound on the bit error probability will be derived. This bound is based on the union bound technique.

CPM schemes do not possess the uniform error property [13] of geometrically uniform codes [14]. Therefore, one can not assume the all zero sequence to be transmitted during the analysis. In fact, CPM belongs to the class of *general codes* [15]. Consequently, the convergence analysis technique, *e.g.*, [16, 17], which was based on geometrically uniform codes has to be modified to adapt to the non-uniform error property of *General codes*.

The main contributions of this work are: 1) the derivation of the analytical upper bound on the error probability for the un-interleaved PRCC/CPM system; 2) the search of the optimal codes for serially concatenated punctured ring convolutional codes with CPM systems.

## II. PUNCTURED CONVOLUTIONAL CODED CPM OVER RINGS

Let  $Z_M$  denote the ring of integers modulo- $M$ . For a rate  $1/n$  nonsystematic ring convolutional encoder,

the generator polynomial matrix is [13]  $G_N(D) = \begin{bmatrix} G^0(D) \\ \vdots \\ G^{n-1}(D) \end{bmatrix}$ , where  $G^i(D) = g_0^i + g_1^i D + \dots + g_m^i D^m$

for  $i \in \{0, \dots, n-1\}$ . The coefficients  $g_j^i$  for  $0 \leq j \leq m$  belong to the set  $\{0, 1, \dots, M-1\}$ . A high rate Punctured Ring Convolutional Code (PRCC) can be obtained by puncturing a parent  $1/n$  ring convolutional code. The operation of puncturing some coded symbols is implemented by using an  $(n \times p)$  puncturing matrix,  $P_{mat}$ , where  $p$  is the puncturing period. Let  $s$  be the total number of transmitted symbols during a puncturing period  $p$ , the coding rate of a PRCC is  $r = p/s$ .

Assume that the trellis of a PRCC is obtained by puncturing a rate  $1/n$  parent convolutional code. Let  $L_s$  be the length of the encoded source sequence. The output of the PRCC encoder is then a sequence of  $M$ -ary codewords, each of length  $n$ . length<sup>2</sup> of the output sequence of the PRCC encoder is  $n \cdot L_s$ . The  $i$ th codeword is  $\mathbf{u}_i = (u_i^1, u_i^2, \dots, u_i^n)$ ,  $u_i^j \in \{0, \dots, M-1\}$ ,  $i \in \{1, \dots, N\}$  and  $j \in \{1, \dots, n\}$ .

## III. RATE ADAPTIVE CODED CPM USING PRCC

We now investigate a punctured trellis coded CPM over the ring of integers modulo  $M$ . The investigated CPM schemes are  $M$ -ary with modulation index  $h = 1/M$ . Both the punctured ring convolutional encoder and the Continuous Phase Encoder (CPE)<sup>3</sup> have the same algebraic structure. A block diagram of the encoder is shown in Fig. 1. The generated waveform from the CPM modulator is transmitted over the channel. The channel is assumed to be the AWGN channel.

The overall channel encoder of the concatenated PRCC/CPM systems is the combined PRCC encoder and the CPE. The CPE takes one output symbol from the PRCC as an input and generates one vector which is used by the memoryless modulator of CPM to generate one channel transmission waveform. Decoding of the combined system can be based on the trellis for trellis coded CPM over rings. A system diagram for the concatenated PRCC/CPM without interleaver is given by Fig. 2.

We now study a symbol-by-symbol *a posteriori* Probability (APP) (or BCJR) decoding algorithm [19] for un-interleaved concatenated PRCC/CPM over the ring of integers modulo- $M$ . It is different from all systems

<sup>1</sup>CPFSK is a subclass of CPM.

<sup>2</sup>Notice that the total length of the output sequence of a PRCC encoder is not related to the rate of the underlying PRCC, but related to the rate of the parent code.

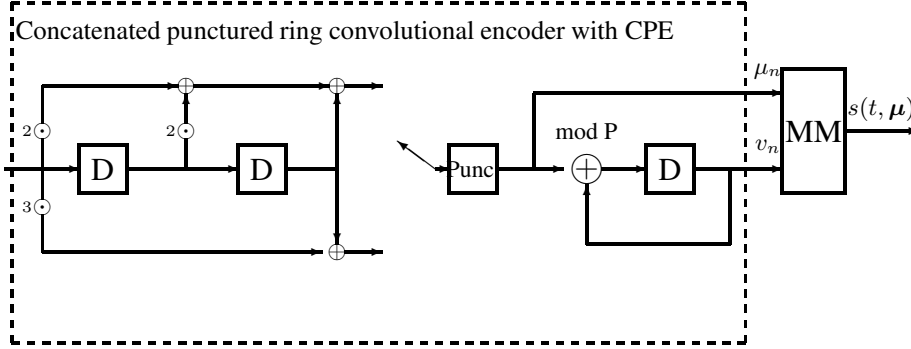


Fig. 1

SYSTEM MODEL FOR THE PUNCTURED RING CONVOLUTIONAL CODED CPM OVER RINGS, THE GENERATOR POLYNOMIAL MATRIX OF THE ENCODER IS  $G(D) = [2 + 2D + D^2; 3 + D^2]$ .

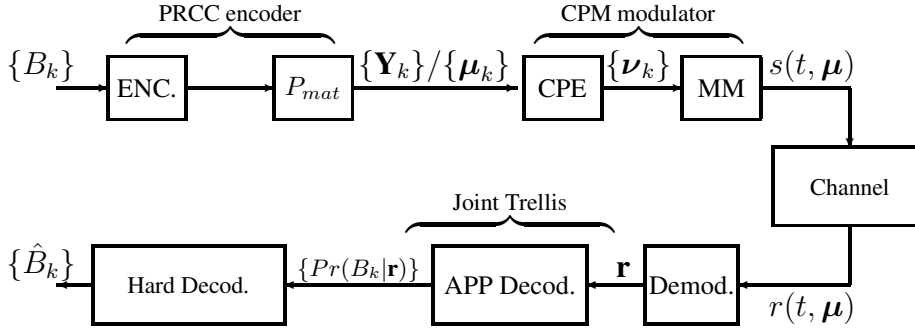


Fig. 2

SYSTEM MODEL FOR A CONCATENATED PRCC/CPM SYSTEM OVER THE CHANNEL.

in the literature so far, *e.g.*, [2, 3], etc. For PRCC/CPM, the decoding is more complicated than that for convolutional coded CPM over rings without puncturing [2, 3]. The reason is that the trellis structure varies for different trellis sections.

For example, consider a combined punctured ring convolutional encoder over  $Z_4$  with  $P_{mat} = [110; 101]$  with a quaternary 1REC<sup>4</sup> CPM with modulation index  $h = 1/4$ . If at time  $k$ , there is no puncturing, (which corresponds to the first column of the puncturing matrix  $P_{mat}$ ), the decoder employing the APP algorithm will determine the transition branch metric based on the two received symbols or waveforms corresponding to the two non-punctured output symbols of the ring convolutional encoder. At time  $k + 1$ , the decoder will determine the metric based on the received symbol corresponding to the non-punctured upper output symbol of the ring encoder. Since the state of the CPE depends on the branch output symbols, the state transitions will be different for different trellis sections.

It is possible to fix the trellis structure for decoding. The decoder can wait until receiving two symbols to decode even for trellis sections with puncturing, that is, the decoding is based on two trellis sections. The

problem, however, is that the concatenated symbols of the two trellis sections are not the output from the ring convolutional encoder with one input symbol. They correspond to two consecutive input symbols of the ring convolutional encoder. It is then hard to determine the state of the concatenated PRCC/CPM.

In this work, the decoding is based on a varying trellis structure. The state  $\sigma_j$  of the trellis at discrete time  $j$  is defined as  $(\sigma_j^{cc}, \sigma_j^{cpm})$ , where  $\sigma_j^{cc}$  and  $\sigma_j^{cpm}$  denote the state of the PRCC and the state of CPE at discrete time  $j$ , respectively. For a concatenated PRCC/CPM system with a punctured ring convolutional encoder over the ring of integers modulo  $M$  having  $m$  memory elements, and an  $M$ -ary CPM scheme with a rational and irreducible modulation index  $h = \mathcal{K}/P$ , the total number of states is  $M^m \cdot P \cdot M^{(L-1)}$ . The state transition  $\sigma_j \rightarrow \sigma_{j+1}$  is determined by the input of the punctured ring convolutional encoder. Associated with this transition is also the input symbol  $\mu \in \{0, \dots, M-1\}$  of the CPE and the mean vector which is obtained by letting the transmitted CPM waveform pass through a bank of complex filters which are matched to the transmitted signals.

The APP decoding algorithm [19] for an un-interleaved coded CPM system computes the APP  $Pr(U_k = \mu | \mathbf{r}_1^\ell)$  of an input symbol  $\mu$  of the CPE at symbol interval  $k$  conditioned on a sufficient statistic  $\mathbf{r}_1^\ell = (\mathbf{r}_1, \dots, \mathbf{r}_\ell)$  based on channel observations  $r(t, \mu)$ , where  $\ell$  is the length of the input data sequence to the CPE.

In [20], we developed an upper bound on the channel distortion<sup>5</sup> for a combined Trellis Coded Quantizer (TCQ) with binary convolutional coded CPM system under MLSD. In this work, we will derive an upper bound on the symbol error probability for the rate adaptive coded CPM system under MLSD. The bound is based on the transfer function technique [21], which is modified and generalized to time variant trellis. This, in turn, is based upon the union bound. It is shown in [20] that the developed analytical bounds are consistent with the simulation results. This method can also be applied to the concatenated PRCC/CPM. Let  $E_s$  be the information symbol energy and  $N_0/2$  be the double sided power spectral density of the additive white Gaussian noise. Let  $m$  be the number of memory elements of the punctured ring convolutional encoder and  $\nu$  the transmission rate in bits per channel symbol. The symbol error probability for a memoryless  $M$ -ary information source sequence of an un-interleaved PRCC/CPM system will follow the following theorem.

*Theorem 1:* Under the MLSD and the assumption that the source block is infinitely long, the symbol error probability for a concatenated PRCC/CPM system with a discrete memoryless uniform digital source sequence, under the assumption that the upper bounds is based on the assumption that the source block is infinitely long, so that the effects caused by the error events across the boundary of the block can be ignored. In the appendix, it was shown that can be upper bounded by

$$P_s < Q \left( \sqrt{d_{min}^2 \frac{E_s r}{\nu N_0}} \right) \exp \left( d_{min}^2 \frac{E_s r}{2\nu N_0} \right) \cdot \frac{\partial \Psi(\eta, \epsilon, \zeta)}{\partial \epsilon} \Big|_{\eta=M^{-\nu}, \epsilon=1, \zeta=e^{-E_s r / 2\nu N_0}}, \quad (1)$$

where  $d_{min}^2$  is the minimum NSED and  $\eta, \epsilon, \zeta$  are dummy variables [21] and  $r$  is the code rate of the trellis encoder of the PRCC,  $r = p/s$  as described in Section II. The average transfer function is

$$\begin{aligned} \Psi(\eta, \epsilon, \zeta) &= M^{-m} \sum_{\kappa=1}^{M^m} \Psi(j, \kappa, \eta, \epsilon, \zeta) \\ &= M^{-m} \frac{1}{p} \sum_{j=0}^{p-1} \sum_{\kappa=1}^{M^m} \sum_{\iota} \sum_{\tau} \sum_d \Theta_{j, s_\kappa, \iota, \tau, d} \eta^\iota \epsilon^\tau \zeta^{d^2} \end{aligned} \quad (2)$$

where  $\Theta_{j, s_\kappa, \iota, \tau, d}$  is the number of error events that start at time  $j$  from state  $s_\kappa$ , and have NSED  $d^2$ , length  $\iota$  and total number of symbol errors caused by the error event given by  $\tau$ . The  $Q$  function is defined as  $Q(x) = (\sqrt{2\pi})^{-1} \int_x^\infty e^{-z^2/2} dz$ .  $\square$

The proof of the above Theorem is given in Appendix A.

The transfer function  $\Psi(j, \kappa, \eta, \epsilon, \zeta)$  can be obtained by using a product state diagram [22, 23]. A product state at time  $j$  is defined as  $(\sigma_j, \hat{\sigma}_j)$ , where  $\sigma_j$  is a state of the encoder of a coded CPM system and  $\hat{\sigma}_j$  represents a state of the decoder. The transition  $(\sigma_j, \hat{\sigma}_j) \rightarrow (\sigma_{j+1}, \hat{\sigma}_{j+1})$  is labeled with

$$\sum_{\Delta\tau} \sum_{\Delta d^2} b(\Delta\tau, \Delta d^2) \eta \epsilon^{\Delta\tau} \zeta^{\Delta d^2}, \quad (3)$$

where  $\Delta\tau$  and  $\Delta d^2$  are the number of the symbol errors and NSED, respectively.  $b(\Delta\tau, \Delta d^2)$  denotes the number of paths having NSED  $\Delta d^2$  and symbol errors  $\Delta\tau$  for this state transition.

*Example III.1:* For a punctured quaternary convolutional encoder with generator polynomial  $(1, D)$  combined with a quaternary 1REC<sup>6</sup> CPM system with  $h = 1/4$ . The number of product states is 64 and the product states range from (0000) to (3333).

For coded CPM over rings, the symbol error rate only depends on the output of the ring convolutional encoder. In other words, it is independent of the pair state of CPM  $(\sigma_j^{\text{cpm}}, \hat{\sigma}_j^{\text{cpm}})$ . Furthermore, the NSED  $d^2$  only depends on the difference of the CPM states  $(\sigma_j^{\text{cpm}} - \hat{\sigma}_j^{\text{cpm}})$  [1]. Therefore, the product state can be reduced. For full response CPM systems [1], the reduced product state can be written as  $(\sigma_j^{\text{cc}}, \hat{\sigma}_j^{\text{cc}}, \omega_j)$ , where the difference phase state  $\omega_j$  is given by

$\omega_j = R_P \{(\sigma_j^{\text{cpm}} - \hat{\sigma}_j^{\text{cpm}})\} = R_P \left\{ \sum_{n=0}^{j-L} \gamma_n \right\}$  is the difference phase state, see (9). The total number of product states for coded CPM with full response CPM systems is  $P \cdot M^{2m}$ .

The product states of ring convolutional coded CPM can be divided into initial states, transfer states and end states. A product state is an initial state if an error event can start from it. A product state is an end state if an error event can end in it. The conditions for initial states and end states are  $\sigma_j^{\text{cc}} = \hat{\sigma}_j^{\text{cc}}$  and  $\omega_j = 0$ . Other states are referred to as transfer states.

*Example III.2:* For the system given in Example III.1, the total number of the reduced product states is 64. The initial states and the end states are the same, and they are (000), (110), (220), (330). The remaining 60 states are the transfer states.

Let  $\xi_{\kappa,j}$  represent the state transitions from an initial state  $s_\kappa$  to transfer states in one step at time  $j$ . Let us denote by  $\Phi_j$  the transitions from transfer states to end states, and by  $\varpi_j$  the transitions from transfer states to transfer states in one step at time  $j$ . Let  $\chi_{\kappa,j}$  represent the transitions from an initial state  $s_\kappa$  to end states in one step. The transfer function can be calculated by [21, 26]

$$\Psi(j, \kappa, \eta, \epsilon, \zeta) = \mathbf{1} \cdot (\Phi_j (\mathbf{I} - \varpi_j)^{-1} \xi_{\kappa,j} + \chi_{\kappa,j}) \quad (4)$$

where  $\mathbf{1}$  is an all one vector and  $\mathbf{I}$  represents the identity matrix.

Equation (1) can be further expressed as

$$P_s \leq \sum_{d^2} \Theta_d \cdot Q\left(\sqrt{d^2 \frac{E_s r}{\nu N_0}}\right), \quad (5)$$

where  $\Theta_d = \frac{M^{-m}}{p} \sum_{j=1}^p \sum_{\kappa=1}^{M^m} \sum_{\iota} \sum_{\tau} \Theta_{j, s_\kappa, \iota, \tau, d} \cdot \mathcal{T} \cdot M^{-\nu \cdot \iota}$ .

It can be seen from (5) that the minimum NSED  $d_{min}^2$  and  $\Theta_{d_{min}}$  (the coefficient of error events with  $d_{min}^2$ ) dominate the asymptotical symbol error rate of the system. For computations of  $\Theta_{j, s_\kappa, \iota, \tau, d}$  and  $\Theta_d$ , we refer the readers to [20, 27]. For a concatenated PRCC/CPM, the NSED  $d^2$  associated with an error event  $\Upsilon = \mu - \mu'$  can be calculated as

$$R \cdot \log_2 M \cdot \left( l - \frac{1}{T} \sum_{i=0}^{l-1} \int_{iT}^{(i+1)T} \cos[2\pi h \omega_i + 4\pi h \sum_{j=i-L+1}^i \gamma_j q(t-jT)] dt \right) \quad (6)$$

$$d^2 = \frac{1}{2E_b} \int_{-\infty}^{\infty} [s(t, \mathbf{U}) - s(t, \hat{\mathbf{U}})]^2 dt$$

$$d^2 = r \cdot \log_2 M \cdot \left( \iota - \frac{1}{T} \sum_{i=0}^{\iota-1} \int_{iT}^{(i+1)T} \cos \phi(t, \gamma) dt \right). \quad (7)$$

Here  $T$  is the symbol interval duration and  $\phi(t, \gamma) = [2\pi h\omega_i + 4\pi h \sum_{j=i-L+1}^i \gamma_j q(t - jT)]$ , where  $\omega_j = R_P \{(\sigma_j^{cpm} - \hat{\sigma}_j^{cpm})\} = R_P \left\{ \sum_{n=0}^{j-L} \gamma_n \right\}$  is the difference phase state and  $r$  is the code rate of the trellis encoder of the PRCC,  $r = p/s$ .  $R_x\{\cdot\}$  is the modulo  $x$  operator and  $q(\cdot)$  is the phase response [1].

Largest  $d_{min}^2$  is used as the design criterion for the selection of the best puncture matrices of the investigated un-interleaved PRCC/CPM systems.

#### IV. SIMULATION RESULTS FOR COMBINED PRCC/CPM

Computer simulations have been performed for rate adaptive PRCC/CPM systems over AWGN channels. Three systems with puncture matrices given by Table 1 are simulated. The PRCC encoders are obtained by puncturing a rate  $1/2$   $Z_4$  parent non-systematic convolutional code with the generator polynomial matrix  $G(D) = [1 + D + D^2; 1 + D^2]$  and  $G = [1 + D^2; 1 + 2D + 2D^2]$ . For un-interleaved PRCC/CPM, the puncturing matrices are given by  $P_{mat}^1$ , which are obtained by an exhaustive search from all of the possible puncturing patterns for the one which gives the largest minimum NSED. The puncturing matrix is given in Octal form, for example,  $(3, 5)_o$  represents the puncture matrix  $[011; 101]$  where 0 corresponds the position that the symbol is punctured. The corresponding  $\Theta_{d_{min}}$  are also given in the Table 1. Also shown in Table 1 is the observation symbol intervals  $N_B$  which is needed to reach the upper bound on the minimum Euclidean distance [1].

Table 1: Punct. matrices for the investigated PRCC schemes.

Parent codes	$G = [1 + D + D^2; 1 + D^2]$			$G = [1 + D^2; 1 + 2D + 2D^2]$		
Code Rate	$R = 1/2$ $p = 1$	$R = 2/3$ $p = 4$	$R = 3/4$ $p = 3$	$R = 1/2$ $p = 1$	$R = 2/3$ $p = 4$	$R = 3/4$ $p = 3$
$P_{mat}^1$	$(1, 1)_o$	$(15, 13)_o$	$(6, 5)_o$	$(1, 1)_o$	$(16, 15)_o$	$(6, 5)_o$
$d_{min}^2$	5.39	6.97	4.73	6.54	7.39	6.68
$\Theta_{d_{min}}$	0.0068	0.0396	0.0703	0.0676	0.0779	0.1758
$N_B$	11	13	6	11	11	16

For each channel SNR value, 200 source blocks with 5000 symbols were used in the simulation. Fig. 3 shows the upper bound and the simulation results of BER performance for the investigated un-interleaved PRCC/CPM systems. It can be seen that the simulation results agree with the upper bound especially when the channel SNR increases. It also shows that the symbol error probability (SER) performance for parent codes is better than the punctured codes. For example, for  $G = [1 + D + D^2; 1 + D^2]$ , at SER of  $10^{-4}$ , a performance gain of roughly  $\sim 2$  dB can be obtained over the rate  $3/4$  system.

#### V. SUMMARY

A rate adaptive coded modulation scheme based on concatenated PRCC/CPM is investigated. The optimal puncturing matrices are presented. Compared with fixed rate convolutional coded CPM over ring, the channel

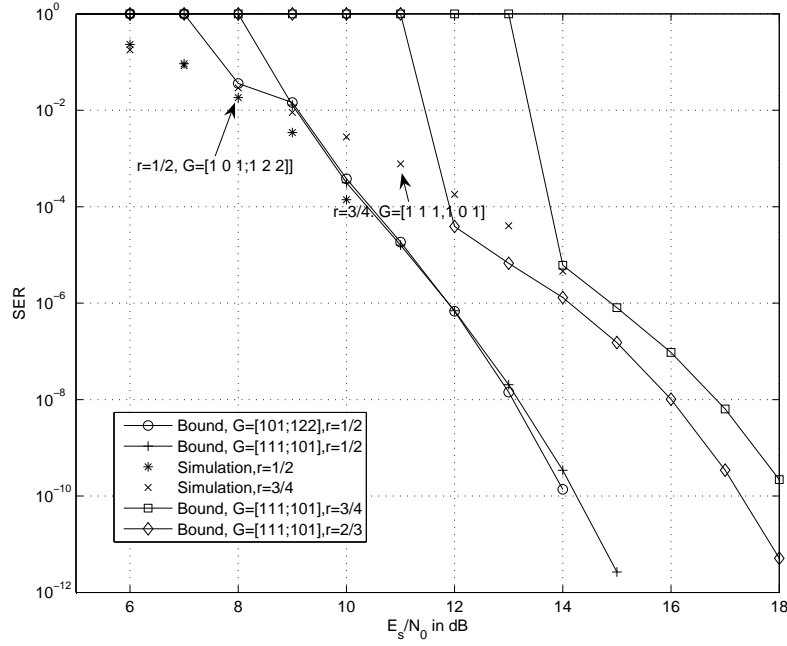


Fig. 3

ANALYTICAL UPPER BOUND AND SOME SIMULATION RESULTS FOR UN-INTERLEAVED PRCC/CPM WITH  $r = 1/2, 2/3, 3/4$ ,  $G = [1 + D + D^2; 1 + D^2]$  AND WITH  $r = 1/2$ ,  $G = [1 + D^2; 1 + 2D + 2D^2]$ .

## APPENDIX A

The proof of the Theorem 1 is given below. The ML sequence detector outputs the decoded source sequence according to

$$\hat{\mathbf{u}} = \arg \max_{\{\mathbf{u}\}} p(\mathbf{r}|\mathbf{u}). \quad (8)$$

where  $\mathbf{u}$  is the source sequence, i.e., the input sequence of the punctured ring convolutional encoder. Let us denote by  $\varsigma_j$  the total symbol error caused by all error events starting at a discrete time  $j$ . Let us take an arbitrary state, say state  $s$ ,  $s \in S$ , where  $S$  is the state space. Let  $\Upsilon_{j,s,\ell,\tau,d}$  be the error event starting at time  $j$  with initial state  $s$ , length  $\ell$ , and Normalized Squared Euclidean Distance (NSED)  $d^2$  [1].  $\tau$  represents the symbol error caused by the error event  $\Upsilon_{j,s,\ell,\tau,d}$ .  $\Upsilon_{j,s,\ell,\tau,d}$  is completely described by the start state  $s$  and the pair sequences  $(\mathbf{u}_{s,\ell}, \hat{\mathbf{u}}_{s,\ell})$ , resulting in  $\Upsilon_{j,s,\ell,\tau,d}$ . Here  $\mathbf{u}_{s,\ell}$  and  $\hat{\mathbf{u}}_{s,\ell}$  are the reconstructed data sequences.

as

$$d^2 = r \cdot \log_2 M \cdot \left( \iota - \frac{1}{T} \sum_{i=0}^{\iota-1} \int_{iT}^{(i+1)T} \cos \phi(t, \gamma) dt \right). \quad (9)$$

Here  $T$  is the symbol interval duration and  $\phi(t, \gamma) = [2\pi h \omega_i + 4\pi h \sum_{j=i-L+1}^i \gamma_j q(t - jT)]$ , where  $\omega_j = R_P \{(\sigma_j^{cpm} - \hat{\sigma}_j^{cpm})\} = R_P \left\{ \sum_{n=0}^{j-L} \gamma_n \right\}$  is the difference phase state.  $R_x\{\cdot\}$  is the modulo  $x$  operator and  $q(\cdot)$  is the phase response [1].

The expected value of the symbol error rate, caused by error events starting at time  $j$ , is given by

$$\begin{aligned} E[\zeta_j] &= \sum_s \sum_\iota \sum_\tau \sum_d \Theta_{j,s,\iota,\tau,d} \cdot \Pr(\Upsilon_{j,s,\iota,\tau,d}) \\ &= \sum_s \sum_\iota \sum_\tau \sum_d \Theta_{j,s,\iota,\tau,d} \cdot \Pr(\hat{\mathbf{U}}_j = \hat{\mathbf{u}}_{s,\iota} | \mathbf{U}_j = \mathbf{u}_{s,\iota}) \cdot \Pr(\mathbf{U}_j = \mathbf{u}_{s,\iota}), \end{aligned} \quad (10)$$

where  $\mathbf{U}_j$  and  $\hat{\mathbf{U}}_j$  are two random vectors, whose outcome space are all possible reconstructed signal sequences starting at time  $j$ .  $\Theta_{j,s,\iota,\tau,d}$  is the number of error events that start with state  $s$ , and have NSED  $d^2$ , length  $\iota$  and total error symbols  $\tau$ . The expectation of (10) is over all error events starting at time  $j$ .

Suppose that the encoding rate of the convolutional encoder over the ring  $Z_M$  is  $k/(k+1)$ . Then there are  $M^k$  branches entering and leaving each state. For a discrete memoryless uniform digital source, all sequences that start with a state  $s$  and have length  $\iota$ , are equally probable. Thus, we can write

$$\Pr(\mathbf{U}_j = \mathbf{u}_{s,\iota}) = \Pr(\sigma_j = s) \cdot M^{-k \cdot \iota}. \quad (11)$$

Let  $\varphi$  be the set of all sequences  $\mathbf{U}_{s,\iota}$  starting at time  $j$  with state  $s$  having length  $\iota$ . Let us denote by  $|\varphi|$  the cardinality of the set  $\varphi$ . When  $|\varphi| = 2$ , there are only two sequences in the set  $\varphi$ ,  $\mathbf{u}_{s,\iota}$  and  $\hat{\mathbf{u}}_{s,\iota}$ . With MLSD, the decision region of  $\hat{\mathbf{u}}_{s,\iota}$  is half of the signal space and the error probability  $\Pr(\hat{\mathbf{U}}_j = \hat{\mathbf{u}}_{s,\iota} | \mathbf{U}_j = \mathbf{u}_{s,\iota})$  is exactly given by  $Q(\sqrt{2d^2 E_b / 2N_0})$ , where  $E_b$  is the transmitted bit energy and  $d^2$  is the NSED between the transmitted signals  $s(t, \mathbf{u}_{s,\iota})$  and  $s(t, \hat{\mathbf{u}}_{s,\iota})$ . The complete signal space squared distance between  $s(t, \mathbf{u}_{s,\iota})$  and  $s(t, \hat{\mathbf{u}}_{s,\iota})$  is given by  $2d^2 E_b$ . the transmitted bit energy  $E_b = E_s r / \nu$ , where  $\nu = \log_2 M$ . Therefore,  $\Pr(\hat{\mathbf{U}}_j = \hat{\mathbf{u}}_{s,\iota} | \mathbf{U}_j = \mathbf{u}_{s,\iota}) = Q(\sqrt{d^2 E_s r / (\nu N_0)})$ . When  $|\varphi| > 2$ , the decision region of  $\hat{\mathbf{u}}_{s,\iota}$  is less than half of the decision space. Therefore,  $\Pr(\hat{\mathbf{U}}_j = \hat{\mathbf{u}}_{s,\iota} | \mathbf{U}_j = \mathbf{u}_{s,\iota}) < Q(\sqrt{d^2 \frac{E_s r}{\nu N_0}})$ . From above, we can conclude that the conditional probability  $\Pr(\hat{\mathbf{U}}_j = \hat{\mathbf{u}}_{s,\iota} | \mathbf{U}_j = \mathbf{u}_{s,\iota})$  can be upper bounded by  $Q(\sqrt{\frac{d^2 E_s r}{\nu N_0}})$ .

With the above result and (11), by considering all error events and using the union bound technique [13],  $E[\zeta_j]$  can be upper bounded by

$$E[\zeta_j] \leq \sum_s \Pr(\sigma_j = s) \sum_\iota \sum_\tau \sum_d \Theta_{j,s,\iota,\tau,d} \cdot M^{-k \cdot \iota} Q\left(\sqrt{d^2 \frac{E_s r}{\nu N_0}}\right). \quad (12)$$

To further reduce the complexity of the computation of (12), one need to note that for a coded CPM, some of the states are equivalent. Here ‘‘equivalent’’ means that if the error events  $\Upsilon_\sigma$  and  $\Upsilon_\rho$ , starting at time  $j$ , generated by the same pair sequences  $(\mathbf{u}_\iota, \hat{\mathbf{u}}_\iota)$  starting at states  $\sigma$  and  $\rho$ , respectively, are identical. Here ‘‘identical’’ means that the error events have the same length, the same NSED, and generate the same number of symbol errors. In the following, we mathematically denote two equivalent states  $\sigma$  and  $\rho$  by  $\sigma \equiv \rho$ ,

Based on the above statement, all the states of the punctured ring convolutional coded CPM at time  $j$ , having the same state of the convolutional encoder,  $\sigma_j^{\text{cc}}$ , are equivalent. Among the  $M^m \cdot P \cdot M^{(L-1)}$  states of the coded CPM, there are only  $M^m$  distinct states which are not equivalent to each other. Consequently, (12) can be written as

$$E[\zeta_j] \leq \sum_{\sigma_j^{\text{cc}}} \Pr(\sigma_j^{\text{cc}} = s_{\sigma_j^{\text{cc}}}) \sum_\iota \sum_\tau \sum_d \Theta_{j,s_{\sigma_j^{\text{cc}}},\iota,\tau,d} \cdot M^{-k \cdot \iota} Q\left(\sqrt{d^2 \frac{E_s r}{\nu N_0}}\right) \quad (13)$$



Let us denote by  $L_T$  the length of the input sequence. Under the assumption that the source sequence is infinitely long, the symbol error probability can be upper bounded by

$$P_s \leq \frac{1}{L_T} \sum_{j=0}^{L_T-1} E[\zeta_j] \leq \frac{1}{L_T} \sum_{j=0}^{L_T-1} \sum_{\kappa=1}^{M^m} Pr(\boldsymbol{\sigma}_j \equiv s_\kappa) \cdot \sum_{\ell} \sum_{\tau} \sum_d \Theta_{j,s_\kappa,\ell,\tau,d} \cdot \tau \cdot M^{-k \cdot \ell} \cdot Q\left(\sqrt{d^2 \frac{E_s r}{\nu N_0}}\right). \quad (14)$$

For an i.i.d. discrete memoryless source, the encoder can start at any one of the  $M^m$  trellis states. Further, since the trellis is periodically time variant,  $E[\zeta_j]$  is periodically dependent on the time  $j$ . The probability that a state  $\boldsymbol{\sigma}_j$  of the coded CPM at time  $j$  is equivalent to one of the  $M^m$  distinct states is

$$Pr(\boldsymbol{\sigma}_j \equiv s_\kappa) = M^{-m}, \quad \forall j. \quad (15)$$

Eq. (14) can then be expressed as

$$P_s \leq \frac{1}{p} \sum_{j=0}^{p-1} M^{-m} \sum_{\kappa=1}^{M^m} \sum_{\ell} \sum_{\tau} \sum_d \Theta_{j,s_\kappa,\ell,\tau,d} \cdot \tau \cdot M^{-k \cdot \ell} \cdot Q\left(\sqrt{d^2 \frac{E_s r}{\nu N_0}}\right), \quad (16)$$

where  $p$  is the puncturing period as described in Section II, and  $j = 0$  corresponding the beginning of a puncturing period.

By using the inequality  $Q(\sqrt{x+y}) \leq Q(\sqrt{x})e^{-y/2}$  for  $x, y > 0$  [1], and letting  $d^2 = d_{min}^2 + (d^2 - d_{min}^2)$ , the above inequality becomes

$$P_s \leq Q\left(\sqrt{d_{min}^2 \frac{E_s r}{\nu N_0}}\right) \exp\left(d_{min}^2 \frac{E_s r}{2\nu N_0}\right) M^{-m} \frac{1}{p} \sum_{j=0}^{p-1} \sum_{\kappa=1}^{M^m} \sum_{\ell} \sum_{\tau} \sum_d \Theta_{j,s_\kappa,\ell,\tau,d} \cdot \tau \cdot 2^{-k \cdot \ell} \cdot \exp\left(-d^2 \frac{E_s r}{2\nu N_0}\right). \quad (17)$$

The right hand side of the above inequality can be computed by means of the generating function. Let us denote by  $\Psi(j, \kappa, \eta, \epsilon, \zeta)$  the generating function for one of the distinct equivalent states  $s_\kappa$ ,  $\kappa = 1, 2, \dots, M^m$ .  $\Psi(j, \kappa, \eta, \epsilon, \zeta)$  is then given by

$$\Psi(j, \kappa, \eta, \epsilon, \zeta) = \sum_{\ell} \sum_{\tau} \sum_d \Theta_{j,s_\kappa,\ell,\tau,d} \eta^\ell \epsilon^\tau \zeta^{d^2} \quad (18)$$

where  $\eta, \epsilon, \zeta$  are ‘‘dummy’’ variables [21]. Using the above equation, Eq. (17) can be written as

$$P_s \leq Q\left(\sqrt{d_{min}^2 \frac{E_s r}{\nu N_0}}\right) \exp\left(d_{min}^2 \frac{E_s r}{2\nu N_0}\right) \cdot \frac{\partial \Psi(\eta, \epsilon, \zeta)}{\partial \epsilon} \Big|_{\eta=M^{-k}, \epsilon=1, \zeta=e^{(-E_s r/2\nu N_0)}}, \quad (19)$$

where the average generating function  $\Psi(\eta, \epsilon, \zeta)$  is given by

$$\Psi(\eta, \epsilon, \zeta) = M^{-m} \frac{1}{p} \sum_{j=0}^{p-1} \sum_{\kappa=1}^{M^m} \Psi(j, \kappa, \eta, \epsilon, \zeta). \quad (20)$$

## REFERENCES

- [1] J. B. Anderson, T. Aulin, and C. E. Sundberg, *Digital Phase Modulation*, Plenum Press, New York, 1986.
- [2] R. H. Yang and D. P. Taylor, ‘‘Trellis-Coded Continuous-Phase Frequency-Shift keying with Ring Convolutional Codes,’’ *IEEE Trans. Inform. Theory*, vol. 40, no. 4, pp. 1057–1067, July 1994.
- [3] B. Rimoldi and Q. Li, ‘‘Coded Continuous Phase Modulation Using Ring Convolutional Codes,’’ *IEEE Trans. Commun.*, vol. 43, no. 11, pp. 2714–2720, Nov. 1995.
- [4] J. L. Massey and T. Mittelholzer, ‘‘Convolutional codes over rings,’’ *Proc. 4th Joint Swedish-USSR Int. Workshop Information Theory*, pp. 14–18, 1989.
- [5] J. L. Massey, T. Mittelholzer, T. Riedel, and M. Vollenweider, ‘‘Ring convolutional codes for phase modulation,’’ *Proc. IEEE Int. Symp. Information Theory*, p. 176, 1990.

- [7] 3GPP TR 25.814 V7.0.0, "Physical Layer Aspects for Evolved UTRA," Tech. Rep., June 2006.
- [8] International Telecommunication Union, *Handbook on Satellite Communications*, A John Wiley & Sons, Inc, third edition, 2002.
- [9] J. Y. Lee, P. Y. Jou, and K. H. Jim and C. E. Kang, "Optimum encoder for trellis-coded cpfsk with ring convolutional codes," *ELECTRONICS LETTERS*, vol. 33, no. 24, pp. 2020–2021, Nov. 1997.
- [10] S. Mahapakulchai and R. E. Van Dyck, "Design of ring convolutional trellis codes for map decoding of mpeg-4 images," *IEEE Trans. Commun.*, vol. 52, no. 7, pp. 1033–1037, July 2004.
- [11] G. D. Forney, Jr., "The Viterbi Algorithm," *Proceedings of the IEEE*, vol. 61, no. 3, pp. 268–278, Mar. 1973.
- [12] M. Xiao and T. Aulin, "Serially concatenated continuous phase modulation with convolutional codes over rings," *IEEE Trans. Commun.*, vol. 54, no. 8, pp. 1387–1395, Aug. 2006.
- [13] A. J. Viterbi and L. K. Omura, *Principles of Digital Communication and Coding*, McGraw-Hill, New York, 1979.
- [14] G. D. Forney, Jr., "Geometrically uniform codes," *IEEE Trans. Inform. Theory*, vol. 37, no. 5, pp. 1241–1260, Sept. 1991.
- [15] S. Benedetto, M. Mondin, and G. Montorsi, "Performance evaluation of trellis-coded modulation schemes," *Proceedings of IEEE*, vol. 82, no. 6, pp. 833–855, June 1994.
- [16] S. ten Brink, "Convergence of iterative decoding," *Electron. lett.*, vol. 35, no. 10, pp. 806–808, May 1999.
- [17] B. Scanavino, G. Montorsi, and S. Benedetto, "Convergence properties of iterative decoders working at bit and symbol level," *Proc. IEEE Global Telecommunications Conference*, vol. 2, no. 25-29, pp. 1037–1041, Nov. 2001.
- [18] B. Rimoldi, "A Decomposition Approach to CPM," *IEEE Trans. Inform. Theory*, vol. 34, no. 2, pp. 260–270, Mar. 1988.
- [19] L. R. Bahl, J. Cocke, F. Jelinek, and J. Raviv, "Optimal decoding of linear codes for minimizing symbol error rate," *IEEE Trans. Inform. Theory*, vol. IT-20, pp. 284–287, Mar. 1974.
- [20] Z. Lin and T. Aulin, "Upper Bounds On The Channel Distortion of Combined TCQ/CPM Systems," in *Proc. of International Conference on Communications*, Seoul, South Korea, May 2005.
- [21] T. Aulin, "Symbol Error Probability Bounds for Coherently Viterbi Detected Continuous Phase Modulated Signals," *IEEE Trans. Commun.*, vol. COM-29, no. 11, pp. 1707–1715, Nov. 1981.
- [22] E. Biglieri, "High-level modulation and coding for nonlinear satellite channels," *IEEE Trans. Commun.*, vol. COM-32, pp. 616–626, May 1984.
- [23] J. Shi and R. D. Wesel, "Efficient computation of trellis code generating function," *IEEE Trans. Commun.*, vol. 52, no. 2, pp. 219–227, Feb. 2004.
- [24] T. Aulin and C. E. Sundberg, "Continuous phase modulation: Part I-Full response signalling," *IEEE Trans. Commun.*, vol. COM-29, pp. 196–209, Mar. 1981.
- [25] T. Aulin, N. Rydbeck, and C. E. Sundberg, "Continuous phase modulation: Part II-Partial response signalling," *IEEE Trans. Commun.*, vol. COM-29, pp. 210–225, Mar. 1981.
- [26] G. Lindell, *On Coded Continuous Phase Modulation*, Ph.D. thesis, Dept. Telecommunication Theory, University of Lund, Sweden, 1985.
- [27] Z. Lin, *Joint Source-Channel Coding using Trellis Coded CPM*, Ph.D Thesis, Chalmers University of Technology, Gothenburg, Sweden, Jan. 2006, <http://www.ce.chalmers.se/TCT>.